

Experiments with Bose-Einstein Condensates on an Atom Chip

**B. Upcroft, C. J. Vale, A. Ratnapala, S. Holt, M. J. Davis,
T. Campey, N. Heckenberg and H. Rubinsztein-Dunlop**

*Centre for Biophotonics and Laser Science, School of Physical Sciences, University of
Queensland, St. Lucia, QLD. 4072, Australia
Phone: +61-7-3346 9425, email: halina@physics.uq.edu.au*

ABSTRACT

We describe the production of BECs on a new type of atom chip based on silver foil. Our atom chip is fabricated with thick wires capable of carrying currents of several amperes without overheating. The silver surface is highly reflective to light resonant with optical transitions used for Rb. The pattern on the chip consists of two parallel Z-trap wires, capable of producing two-wire guide, and two additional endcap wires for varying the axial confinement. Condensates are produced in magnetic microtraps formed within 1 mm of surface of the chip. We have observed the fragmentation of cold atom clouds when brought close to the chip surface. This results from a perturbed trapping potential caused by nanometer deviations of the current path through the wires on the chip. We present results of fragmentation of cold clouds at distances below 100 μm from the wires and investigate the origin of the deviating current. The fragmentation has different characteristics to those seen with copper conductors. The dynamics of atoms in these microtraps is also investigated.

Key words: Atom optics, Atom chips, Bose-Einstein condensate

INTRODUCTION

Since the advent of laser cooling of neutral atoms with the combination of counterpropagating laser beams and magnetic fields, there have been some significant advances in the preparation of cold atomic samples. One of the major breakthroughs was the observation of a Bose-Einstein condensate (BEC) in a gaseous cloud of rubidium atoms¹. Laser cooling and the formation of a BEC enabled the production of coherent matter which in many ways is analogous to light produced by a laser. The observation of BEC has led to very rapid developments in the field of atom optics and has encouraged physicists to study the behaviour of atoms at these tremendously low temperatures, probing the fundamentals of nature and the fascinating world of quantum mechanics². Conventional magnetic traps used for producing BEC consist of current carrying coils external to the vacuum chamber containing the atoms. To create magnetic traps tight enough to achieve a high collision rate needed for evaporative cooling, the coils need large stable currents passed through them. This intrinsically decreases the flexibility of the experiment as the magnetic potentials are hard to manipulate spatially and temporally. Therefore the nature of magnetic traps which confine the BECs are limited in the degree to which the atoms can be controlled. The advantages of conventional traps is that they have been around since the first Bose-Einstein condensate and have been refined over a number of years. These traps also allow BECs with a large number of atoms to be routinely produced. However, the limited control using the conventional experimental apparatus for both thermal atomic clouds and BEC's was an incentive for some groups to find alternatives to the standard atomic traps (including the magneto-optical trap (MOT)) and the secondary magnetic traps needed to transform the thermal cloud of atoms into a BEC. The alternative traps needed freedom for the manipulation of atomic samples both in their thermal state and as a BEC. In order to obtain better spatial and temporal control, the magnetic traps were miniaturised and brought closer to the atoms.

The electronics world has seen the miniaturisation of components and the success this has brought. Components are reaching sizes in which only single electrons can pass through the wires at a time³. This miniaturisation has led to many powerful devices including the microprocessor. Miniaturisation has also occurred in the optics world with microscopic lasers and optical elements being produced on silicon substrates^{4,5}. The flexibility of silicon based

electronics and optics can also be transferred to the atom optics world. The accurate manipulation of neutral atoms at the microscopic level has uncovered new possibilities in quantum information, quantum statistics, the microscopic interactions of bulk surfaces, and the ease of preparing atomic samples^{6,7}.

Atom chip BEC experiments have mostly been performed with chips fabricated using photolithographic techniques⁸⁻¹⁰. These chips have been highly successful and form the basis of a growing number of experiments. However, there are some limitations to chips produced in this manner. One is that the photoresist thickness and etching process constrain the maximum height of the conducting wires. Typical conductor thicknesses range from about 2 μm for evaporatively or sputter-coated wires, up to 10 μm for electroplated wires. The latter also appear to suffer from rough edges, leading to fragmentation of clouds near the surface¹¹. A desirable feature of atom chips is that narrower wires result in tighter trapping potentials near the surface for a fixed current. However, the cross-sectional area (and hence the thickness) of a wire restricts the maximum current that can be sustained before it overheats and detaches from the surface. Current densities of order 10^6 A cm^{-2} have been achieved on atom chips at currents of order 1 A, but continuous operation at these current densities is fraught with danger. An elegant solution to this problem would be to use high- T_c superconducting wires, although this introduces additional technical complexity. Thicker extruded wire¹² and machined copper conductors¹³ have also been used to obtain higher currents, but these methods are not suited to sub-millimetre patterning.

Here we describe a method of fabricating atom chips with thick wires capable of carrying currents of several amperes without overheating. We begin by reviewing magnetic microtraps. We then describe the fabrication process for our chip and demonstrate its effectiveness by using it to produce a Bose-Einstein condensate of ⁸⁷Rb. Finally, cold atom cloud is trapped close to the chip surface and we observe fragmentation of the atomic density profile.

MAGNETIC MICROTRAPS

When an atom with a magnetic dipole moment, μ , is placed in a magnetic field, \mathbf{B} , it experiences an interaction potential $U = -\mu \cdot \mathbf{B}$. If the projection of the magnetic moment onto the field remains constant during the atom's motion, the adiabatic condition is satisfied (i.e. the atom remains in the same magnetic substate, m_F). In such cases the potential is given by the scalar expression, $U = -m_F g_F \mu_B B$, where g_F is the Landé g-factor, μ_B is the Bohr magneton and $B = |\mathbf{B}|$. Atoms whose magnetic moments align antiparallel to \mathbf{B} are known as weak-field seekers, as their lowest energy state is at a minimum of B .

Several arrangements of wires have been proposed¹⁴ and used in experiments to realize a variety of magnetic trapping geometries for weak-field seeking atoms^{7, 15}. A building block for all of these is the 'side guide', in which the combination of the field of a straight conducting wire and homogeneous bias field produces a two-dimensional, linear (to first order) trapping potential (see figure1).

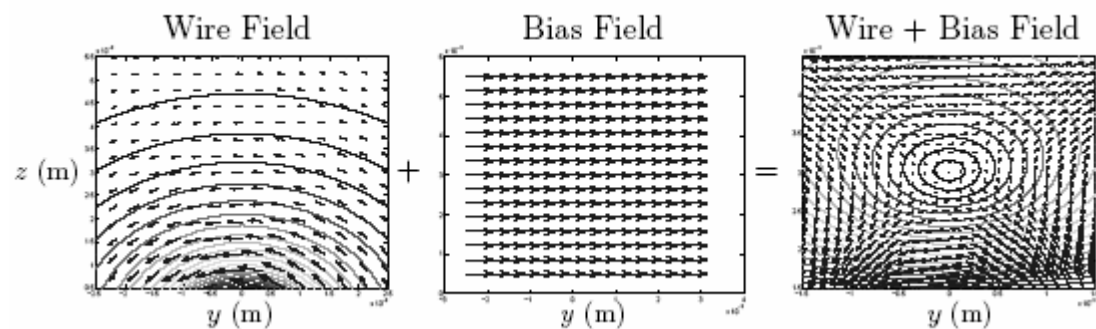


Figure1: The wire quadrupole field (right hand side) is produced by the combination of the magnetic fields from a current carrying wire (left hand side) and an external bias field (centre).

A simple three-dimensional trap can be realized by bending a single wire into the shape of a Z, as shown in figure 2, where the top and bottom wire sections produce a confining potential in the longitudinal (z) direction.

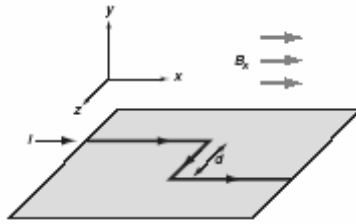


Figure 2: A miniature Ioffe–Pritchard trap on an atom chip. A Z-shaped wire and homogeneous bias field can produce a simple trap for weak-field seeking atoms the middle section of the wire.

The combination of a Z-shaped wire and transverse bias field, B_x , produces a Ioffe–Pritchard type trap with a nonzero minimum located above the centre of the middle section of wire. In the x – y plane the trap minimum is where the field of the wire is exactly compensated by the bias field B_x . While the x and y components of the field go to zero here, the z -component, B_z , is nonzero out of the plane of the chip ($y = 0$), as the fields due to the two sections of current in the x -direction add constructively (see figure 3).

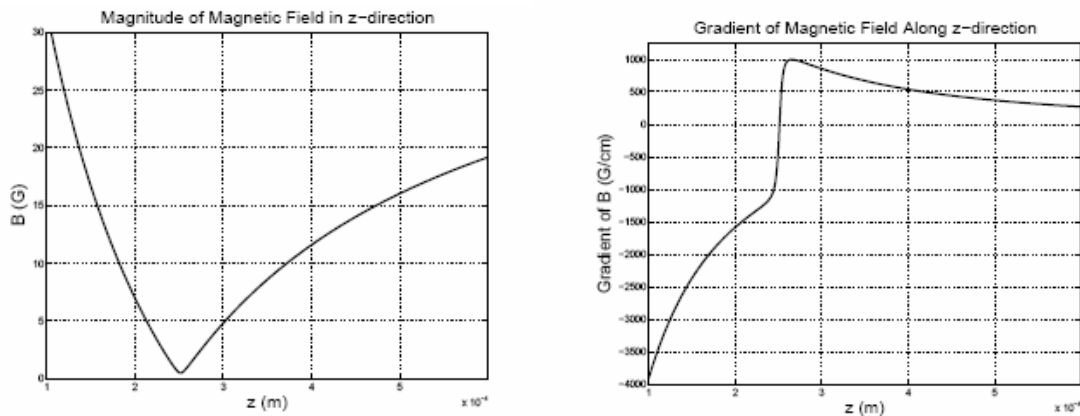


Figure 3: *Left* - magnitude of the magnetic field of the Z-trap in the radial direction. The parameters used were 6A through the Z-wire and 36.5 G bias field. For these parameters the minimum of the trap is approximately 250 μm from the centre of the wire and is approximately 0.5G in magnitude. The trapping frequency in the radial direction is approximately 1.5 kHz and in the axial direction about 30Hz. *Right* – gradient of the Z-trap in the radial direction for the above parameters, where the finite thickness and shape of the wires have been taken into account.

The gradient of a magnetic field indicates how tight a trap is. The tighter the field, the more compressed the atomic cloud, which in turn causes more collisions increasing the efficiency of evaporative cooling. A conventional coil configuration for a Ioffe-Pritchard trap can produce gradients of approximately 180 G/cm in the radial direction. A miniature Z-trap, as described in the experiment, however, is capable of producing 1kG/cm radially (figure 3 right)) for a trap minimum 250 μm from the wire.

The tightness of the trap can also be characterised by the trapping frequencies. They are calculated by considering the atoms as classical particles oscillating in a harmonic potential. The frequency at which they oscillate is the trapping frequency. Note that the Ioffe-Pritchard trap can only be considered harmonic for small deviations from the centre. Hotter atoms will explore the linear section of the trap and the oscillations will be damped. The radial trapping frequency of the Z-trap, using 6A through the Z-wire and 36.5 G bias field, is 1.5 kHz and the axial trapping frequency is 30 Hz.

ATOM CHIP

The atom chip was fabricated entirely in-house using materials and machinery readily available to typical laboratories. A schematic of the chip is shown in figure 4.

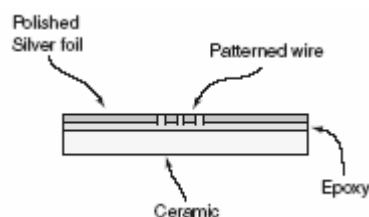


Figure 4: Schematic of the atom chip. A silver foil is glued onto a ceramic substrate using UHV compatible epoxy. The polished foil is approximately $90\ \mu\text{m}$ thick and the epoxy layer is about half this thickness. Insulating channels are cut into the foil with a micro-mechanical cutter and the channels are back-filled with epoxy.

A $125\ \mu\text{m}$ silver foil (Goodfellow AG000360) is glued onto a 1 mm thick machinable ceramic (macor) substrate using EpoTek H77 ultra high vacuum (UHV) compatible epoxy. Silver was chosen as the conductive material as it has the lowest resistivity of all metals ($1.59\ \mu\Omega\ \text{cm}$), compared with gold ($2.2\ \mu\Omega\ \text{cm}$) and copper ($1.67\ \mu\Omega\ \text{cm}$). It is also highly reflective (97%) to light resonant with the Rb D2 transition at 780 nm. The epoxy adheres strongly to the ceramic, but less effectively to the silver. Improved bonding to the silver is achieved by roughening the surface to be glued with fine-grade sand paper. A 100 nm platinum layer is evaporatively coated onto the foil, which is then oxidized (with heat in air) before gluing. After curing the epoxy, the foil is polished to a mirror finish in three stages. Firstly, fine-grade abrasive paper held on a flat block is used under running water to take out any large ($>10\ \mu\text{m}$) ripples in the surface. Secondly, a range of finer grade abrasive cloths (Micromesh 1500–8000) are used down to a grain size of $3\ \mu\text{m}$. Finally, $3\ \mu\text{m}$ and $1\ \mu\text{m}$ grain size diamond polishing pastes (ProSciTech M23/3 and M23/1) are applied to the surface with a silk polishing cloth. These three polishing stages typically remove about $30\text{--}40\ \mu\text{m}$ of the silver, leaving a final conductor thickness of approximately $90\ \mu\text{m}$. The finished surface had very few scratches visible to the naked eye. In order to verify this a near-infrared laser beam is reflected from the finished surface and viewed several metres away without visible distortion. The power in the reflected beam was $95 \pm 2\%$ of the incident power, in good agreement with the known reflectivity of silver at 780 nm.

The polished chip is then ready to be machined. A computer numerically controlled (CNC) milling machine is used to cut insulating gaps into the silver foil using a $150\ \mu\text{m}$ diameter PCB cutting tool (LPKF 0.15 mm end mill, 107244). The wire patterns are programmed into the CNC mill and the cutting performed in several runs, with the cut depth incremented by $20\ \mu\text{m}$ each run. The cutting tool spins at 10 krpm and traces the pattern of the wires at a speed of $5\ \text{mm}\ \text{min}^{-1}$. Small holes ($1\ \text{mm}$ diameter) are drilled through the foil, epoxy and macor near the edges of the chip, in the centre of the current connection pads.

After the pattern is cut, the resulting insulating channels are carefully backfilled with epoxy to provide additional mechanical support and heatsinking for the wires. Finally, the whole chip is repolished using the diamond pastes to remove any scratches or residues from the cutting process. The chip is cleaned with distilled water and methanol before the electrical connections are assembled and the chip is placed in the vacuum chamber.

The robust nature of our chip allows simple yet secure electrical connections to the wires. The holes drilled through the connection pads accommodate 1 mm diameter screws. Copper tabs, also with holes drilled through them, are placed onto the connection pads and held in place by screws with a nut and sprung washer that prevented loosening during bake-out of the vacuum system. By contacting over a large area of the pad we ensure very low resistance connections and negligible heating. Figure 5 shows the completed chip with the electrical connections in place. The copper tabs are attached to barrel connectors, which in turn connect to thicker ceramic coated wires (Kurt J Lesker, CCWA10SI and CCWA20SI) that run to the electrical feedthroughs for the vacuum chamber. Also visible is the rubidium dispenser, attached to the side and recessed by a few millimetres from the silver surface of the chip.



Figure 5: Photograph of the atom chip. The electrical connections via the copper tabs are visible on the four corners of the chips. The rubidium dispenser can be seen on the left side of the chip mount.

We have tested the current-carrying capacity of the chip wires and found that individual wires can sustain currents of 8 A *in vacuo* for 10 s with the temperature remaining below 100 °C. The temperature was evaluated by monitoring the resistance of the wire from outside the vacuum chamber. This necessarily includes the resistance of the connections and connecting wires - our estimate of the heating assumes that the increase in resistance observed was entirely due to heating of the chip wires. We therefore obtain an upper limit for the temperature increase of the chip. A nude ion gauge located approximately 30 cm from the chip could detect no increase of the pressure in the vacuum chamber at the level of 2×10^{-11} mbar during these measurements. The current density in the wire was 5×10^4 A cm⁻².

Figure 5 also shows the wires patterned onto the chip. These consist of two parallel Z-trap wires with a centre-to-centre separation of $2a = 0.4$ mm, and two additional endcap wires for varying the axial confinement. The parallel Z-wires are capable of producing fields suitable for realizing the two-wire guide proposed in¹⁶. Assuming equal currents in the two wires, there are three possible configurations in the x - y plane. These can be selected by the strength of the (dimensionless) bias field, $\beta = B_x/B_0$, where $B_0 = \mu_0 I/2\pi a$. The first configuration, with $\beta < 1$, consists of two quadrupole traps in the $x = 0$ plane, separated vertically by $2a\sqrt{1-\beta^2}/\beta$. The second is a single hexapole trap which occurs at the critical bias field value ($\beta = 1$), with a minimum at $(x, y) = (0, a)$. The third configuration is for $\beta > 1$ and produces two symmetric traps separated horizontally by $2a\sqrt{1-\beta^2}/\beta$. In the axial direction there is only one trapping configuration, as the atoms are much further away from the two end-cap wire sections than the wire separation.

EXPERIMENT

We have used our atom chip to produce Bose–Einstein condensates of ⁸⁷Rb atoms. The experiment follows the usual stages for BEC production and the details of our procedure are described below.

The vacuum chamber consists of a glass cell (made in our glass-blowing workshop) attached to a stainless steel vacuum chamber. We use a 75 l s⁻¹ ion pump and a nonevaporable getter to reach pressures below 2×10^{-11} mbar. This was achieved by baking the chamber for two weeks at a temperature of 140 °C and pumping it with a turbo pump. The epoxy bonding the silver to the ceramic is rated to 150 °C which limits the bake-out temperature.

Rubidium vapour is obtained from a dispenser source which is pulsed with a current of 7.2 A for 12 s. We collect 10^8 atoms in a reflection magneto–optical trap (MOT) formed 4.5mm from the surface of the chip. Trapping light is provided by a Toptica DLX 110 400mW external cavity diode laser system sent through a single mode fibre. It is tuned 15 MHz below the $5S_{1/2} F = 2$ to $5P_{3/2} F = 3$ transition in ⁸⁷Rb. Four trapping beams enter the chamber, each with a power of 23 ± 1 mW and $1/e^2$ diameter of approximately 25 mm. The repump laser is a home-built external

cavity diode laser system locked to the $F = 1$ to $F' = 2$ transition. This laser is combined with the trapping laser on a polarizing beam splitter cube, and approximately 10 mW of repump light enters the chamber.

After the dispenser pulse, atoms are held in the MOT for a further 10 s to allow the vacuum to recover. At this distance from the surface the MOT does not appear to be seriously depleted by the imperfections in our mirror due to the insulating gaps. While we cannot make a direct comparison with aMOT with a near perfect mirror, our atom number (10^8), temperature (90 μ K) and lifetime (40 s) are sufficient for producing condensates.

Next, the atoms are transferred to a compressed MOT with a magnetic field provided by a U-shaped wire centred 1.6 mm below the silver surface carrying a current of 20 A, combined with a uniform transverse bias field of 12 G. This results in a spherical quadrupole field with gradients of 35 G cm^{-1} radially and 5 G cm^{-1} axially leading to an elongated cloud at a distance of 1.5 mm from the chip surface. The MOT lasers and current through the U-wire are then turned off simultaneously in less than 100 μ s and the atoms are optically pumped into the $F = 2$, $m_F = 2$ ground state in 400 μ s. A current of 4 A is then turned on through both Z-wires on the chip and the atoms are caught in the potential produced by the wire and a 12 G transverse bias field. The bias is ramped linearly from 12 G to 30 G over 500 ms to compress the cloud and achieve final trapping frequencies of 570 Hz radially and 11.2 Hz axially at a distance of 430 μ m from the surface. The lifetime of atoms in the magnetic trap is more than 30 s, indicating that the vacuum is not adversely affected by the chip. At this point efficient evaporative cooling can begin.

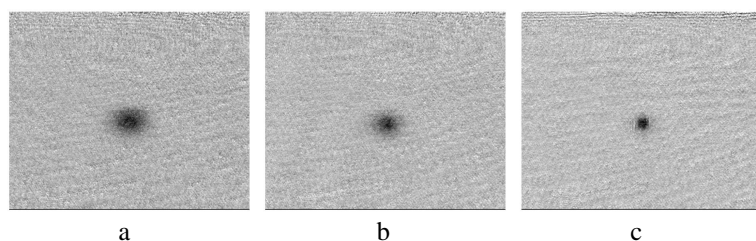


Figure 6: Absorption images after 15 ms free expansion of (a) a thermal cloud at 700 nK, (b) a partially condensed cloud at 450 nK, and (c) an almost pure BEC below 250 nK. A condensate forms below the critical temperature of about 500 nK. The chip wires are visible at the top of the images.

The atomic cloud is evaporatively cooled through the BEC transition using a single logarithmic sweep of a radio frequency (RF) magnetic field from 13 MHz to around 1 MHz in 10.5 s. In the two-wire trap this produces condensates of around 3×10^4 atoms. Larger condensates can be produced by further compressing the cloud into a trap formed by current through a single wire. Figure 6 shows absorption images of atom clouds following 15 ms free expansion after being released from a single wire magnetic trap. The three images show clouds after terminating the RF evaporation at 1080 kHz, 1050 kHz and 1010 kHz respectively, in a trap with an offset field of 1.4 G. The trap forms 200 μ m from the chip surface with oscillation frequencies of 1100 Hz radially and 6 Hz axially. The condensate contains around 5×10^4 atoms and has a peak density of $4 \times 10^{14} \text{ cm}^{-3}$. With our parameters the critical temperature for condensation is around 500 nK, which is reached with approximately 1.2×10^5 atoms.

FRAGMENTATION

When cold atom clouds are brought close to current-carrying wires, the atomic distribution is seen to fragment into ‘lumps’¹⁷⁻¹⁹. This is apparently due to microscopic deviations in the direction of current flow which produce small components of magnetic field parallel or antiparallel to the axis of the wire¹⁷. This effect may prove to be a limitation of current-carrying wire-based atom chips for applications such as atom interferometry.

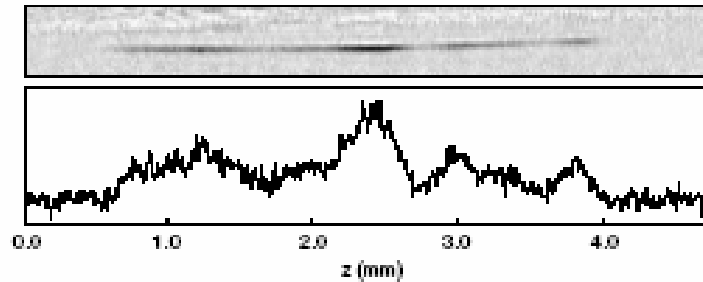


Figure 7: Absorption image (top) and cross-sectional profile (bottom) of a 4 μ K fragmented atom cloud prepared at a distance of 45 μ m from the chip. The trap was accelerated away from the surface for 5 ms before imaging.

We also observe fragmentation of cold clouds brought close to the chip surface. Figure 7 shows an absorption image and an averaged cross-sectional profile of a fragmented atom cloud after being accelerated away from the chip surface. The cloud was prepared at a distance of $45 \pm 5 \mu\text{m}$ from a single wire at a temperature of 4 μK . At this distance the atoms could not be directly viewed in the trap due to light scattered from the gaps between the wires. Therefore the atoms were accelerated away from the surface for 5 ms by ramping up the current through the wire immediately before being imaged. Because of the short acceleration time and the low cloud temperature and axial trapping frequency (nominally 2.9 Hz), any redistribution of atoms in the axial direction in the displaced trap is not significant in the image.

We observe larger structure in the atomic density profile than has been seen in other experiments - up to the millimetre scale. The cross-sectional profile also reveals shorter wavelength structure superposed on these larger fragments. This may be caused by slight deviations in the movement of the cutter during milling producing wires that are not perfectly straight - however we have no direct evidence of this as yet. The depth of the fragmenting potential is comparable to what has been seen above copper conductors^{11,17-19}.

Fragmentation appears to be highly dependent on the geometric and material properties of the conductors¹¹. Our method of chip fabrication may be beneficial in this regard, as the high-purity solid metal foil should have superior conductor uniformity to electroplated wires. It remains to be seen how precisely wires can be patterned into a solid foil, and subsequently how this affects fragmentation. This topic will be investigated in future work. Regardless of any improvements in uniformity, our higher current-carrying capacity allows us to produce moderately tight traps further away from the conductors. This is important as fragmentation is seen to scale approximately as e^{-ky}/ky , where k is the wavenumber of the current deviations^{11,19}.

CONCLUSIONS

We have demonstrated a novel method of producing atom chips suitable for the production and manipulation of Bose–Einstein condensates. Our chip is capable of sustaining higher currents, than typical lithographically patterned chips, and can therefore produce deeper magnetic traps. This facilitates condensate production without sacrificing the versatility of the atom chip. The patterning of wires on our chip is currently at the 100 μm scale but could be reduced using laser cutting to produce the insulating channels. Nonetheless, our technique has proven to be simple and reliable. Because of the higher current-carrying capacity of this set-up, we are able to produce moderately tight traps at distances greater than 100 μm from the surface, where fragmentation effects become less important.

REFERENCES

1. M. Anderson, J. Ensher, M. Matthews, C. Wieman, and E. Cornell. "Observation of Bose-Einstein condensation in a dilute atomic vapour" *Science* **269**, 198 (1995).
2. K. Southwell ed. "Ultracold matter." *Nature Insights* **416**, 2005 (2002).
3. M. Kelly, *Low Dimensional Semiconductors* (Oxford University Press 1995).

4. Y. Kawabe, C. Spiegelberg, A. Schülzgen, M. Nabor, E. Marsh, P. Allemand, M. Kuwata-Gonokami, K. Takeda, and N. Peyghambarian. "Whispering-gallery-mode microring laser using a conjugated polymer". *Appl. Phys. Lett.* **72**, 141 (1998).
5. C. Bauer, H. Giessen, B. Schnabel, E. Kley, C. Schmitt, U. Scherf, and R. Mahrt. "A surface emitting circular grating polymer laser" *Advanced Materials* **13**, 1161 (2001).
6. J. Reichel. "Applications of integrated magnetic microtraps". *Appl. Phys. B: Lasers and Optics* **72**, 81 (2001).
7. R. Folman, P. Krüger, J. Schmiedmayer, J. Denschlag, and C. Henkel. "Microscopic atom optics: From wires to an atom chip" *Advances in Atomic, Molecular, and Optical Physics* **48**, 263 (2002).
8. W. Hänsel, J. Reichel, P. Hommelhoff and T. Hänsch "Applications of integrated magnetic microtraps" *Appl. Phys. B* **72** 81 (2001).
9. J. Fortágh, H. Ott, G. Schlotterbeck, C. Zimmermann, B. Herzog and D. Wharam "Microelectromagnets for trapping and manipulating ultracold atomic quantum gases" *Appl. Phys. Lett.* **81** 1146 (2002).
10. A. E. Leanhardt, Chikkatur, D. Kielpinski, Y. Shin, T. L. Gustavson, W. Ketterle and D. E. Pritchard. "Propagation of Bose-Einstein Condensates in a Magnetic Waveguide" *Phys. Rev. Lett.* **89** 040401, (2002).
11. J. Estève, C. Aussibal, T. Schumm, C. Figl, D. Mailly, I. Bouchoule, C. Westbrook and A. Aspect. "The role of wire imperfections in micro magnetic traps for atoms" *Preprint physics/0403020* (2004).
12. M. P. A. Jones, C. J. Vale, D. Sahagun, B. V. Hall and E. A. Hinds. "Spin Coupling between Cold Atoms and the Thermal Fluctuations of a Metal Surface" *Phys. Rev. Lett.* **91** 080401 (2003).
13. S. Schneider, S. Kasper, Ch. vom Hagen, M. Bartenstein, B. Engeser, T. Schumm, I. Bar-Joseph, R. Folman, L. Feenstra and J. Schmiedmayer. "Bose-Einstein condensation in a simple microtrap" *Phys. Rev. A* **67**, 023612 (2003).
14. J. D. Weinstein and K. G. Libbrecht. "Microscopic magnetic traps for neutral atoms" *Phys. Rev. A* **52**, 4004 (1995).
15. E. A. Hinds and I. G. Hughes. "Magnetic atom optics: mirrors, guides, traps, and chips for atoms" *J. Phys. D: Appl. Phys.* **32** R119 (1999).
16. E. A. Hinds, C. J. Vale and M. G. Boshier "Two-Wire Waveguide and Interferometer for Cold Atoms" *Phys. Rev. Lett.* **86** 1462, (2001).
17. S. Kraft, A. Günther, H. Ott, D. Wharam, C. Zimmermann and J. Fortágh. "Anomalous longitudinal magnetic field near the surface of copper conductor" *J. Phys. B: At. Mol. Opt. Phys.* **35** 469 (2002).
18. A. E. Leanhardt, Y. Shin, A. P. Chikkatur, D. Kielpinski, W. Ketterle and D. E. Pritchard. "Bose-Einstein Condensates near a Microfabricated Surface" *Phys. Rev. Lett.* **90**, 100404 (2003).
19. M. P. A. Jones, C. J. Vale, D. Sahagun, B. V. Hall, C. C. Eberlein, B. E. Sauer and E. A. Hinds. "Cold atoms probe the magnetic field near a wire" *J. Phys. B: At. Mol. Opt. Phys.* **37** L15, (2004).